KEK-79-8
May 1979
A

ACCELERATION OF POLARIZED PROTONS IN THE KEK 500 MeV BOOSTER SYNCHROTRON

Masaaki KOBAYASHI

NATIONAL LABORATORY FOR HIGH ENERGY PHYSICS
OHO-MACHI, TSUKUBA-GUN
IBARAKI, JAPAN

KEK Reports are available from

Technical Information Office
National Laboratory for High Energy Physics
Oho-machi, Tsukuba-gun
Ibaraki-ken, 300-32
JAPAN

Phone: 0298-64-1171
Telex: 3652-534 (Domestic)
(0)3652-534 (International)
Cable: KEKOHO

ACCELERATION OF POLARIZED PROTONS IN THE KEK 500 MeV BOOSTER SYNCHROTRON

Masaaki KOBAYASHI

National Laboratory for High Energy Physics

Oho-machi, Tsukuba-gun, Ibaraki, Japan

Abstract

Acceleration of polarized proton beam is studied by computing the spin as well as orbit motion step by step throughout the whole acceleration period. Acceleration is feasible without or with a ν_z-jump technique.

Without a ν_z-jump technique, the vertical polarization will change the sign with a small loss (2 %) at 239 MeV, the only one intrinsic resonance, if the vertical beam radius is 10 mm at the resonance. Though synchrotron oscillation may cause an additional polarization loss, it will be much less than 10 %.

If a ν_z- jump technique is employed, the initial polarization is maintained including the sign. The depolarization will be as small as 6 % by pulsing 10 cm thick quadrupole magnets added on both ends of each straight section up to 0.1 kGauss/cm within 3 μsec. In this case the influence of synchrotron oscillation is negligibly small.

1. Introduction

In strong focusing proton synchrotrons (PS), the intrinsic depolarizing resonances are sometimes so strong[1)] that the initial polarization of the beam is easily lost unless a technique of fast crossing[2)] is employed at the resonance.

The KEK 500 MeV booster PS has only one resonance at 239 MeV corresponding to a condition

$$\gamma G = \nu_z \ . \qquad (1)$$

Here γ is the conventional Lorentz factor of particles ($\gamma = (1 - \beta^2)^{-1/2}$; β = the particle velocity in units of the light velocity), $G = g/2 - 1 = 1.7928$ the anomalous magnetic moment of protons in nuclear magnetons, and $\nu_z = 2.25$ the vertical betatron wave number.

Khoe[1)] and Sasaki[3)] examined depolarization problems in the KEK booster PS and gave the following predictions based on an approximate analytical estimate:

(i) Complete depolarization occurs.

(ii) In order to reduce the depolarization to $\Delta P/P_0 = 0.1$, ν_z has to be quickly changed by 0.21 within 1 μsec.

(iii) The depolarization resonance can be avoided by

(a) changing ν_z from 2.25 to 1.75,

(b) transfering the booster beam into the 12 GeV main PS at 200 MeV or (c) injecting the linac beam directly into the 12 GeV PS by skipping the booster PS.

Methods avoiding the resonance require significant mechanical changes in the machine construction and therefore we will not consider them here.

It has been predicted[1,4,5)] that without a ν_z-jump technique the initial polarization only changes the sign without reducing much the magnitude if the resonance is strong and/or crossed slowly. This prediction has been recently studied in more detail.[6)]

In order to study the above possibility, we have traced the spin as well as the orbit motion step by step throughout the whole acceleration period. As analytical solutions are used for the spin equation of motion, no serious accumulation of errors in the length of spin vector occurs such as was experienced[7,8)] before if numerical integration was employed.

The result of computation verifies the above possibility if synchrotron oscillation is neglected. Though the synchrotron oscillation may sometimes have a damaging effect on the complete spin flip, the effect is much smaller than 10 %.

If a ν_z-jump technique is employed by quickly pulsing additional quadrupole magnets at the resonance, the depolarization will be as small as 6 %, showing that this is another possibility of accelerating polarized beams at the present PS.

2. Equation of Spin Motion

Let us employ a turing rest frame of particles, which is moving with particles and has its one of the axis (y) always on the equilibrium orbit. The z-axis is always vertical if we assume the equilibrium orbit in a horizontal plane by neglecting the distortion. The x-axis is always radial (see Fig. 1).

The present reference frame resembles in bending magnets to the rotating rest frame of particle except the fixed z axis and in the straight sections to the inertial rest frame respectively. Let us call it simply the turning rest frame. We use mostly the time $t^{(R)}$ in the rest frame rather than the laboratory time $t^{(L)} = \gamma t^{(R)}$.

The equation of spin motion in the turning rest frame can be found by starting from the Froissart-Stora equation[9] established in the laboratory frame:

$$\frac{d\vec{s}}{dt^{(L)}} = \frac{e}{m\gamma}\vec{s} \times \{(1 + G)\vec{B}_y^{(L)} + (1 + \gamma G)(\vec{B}_x^{(L)} + \vec{B}_z^{(L)})\} \tag{2}$$

where $\vec{s}$ is the spin vector of unit length, m the proton rest mass and $\vec{B}^{(L)}$ the laboratory magnetic flux density.

In moving to the turning rest frame, the coefficient for $\vec{B}_z^{(L)}$ has to be changed. For bending magnets, the coefficient is changed from $1 + \gamma G$ to γG by subtracting the angular velocity of $e\langle\vec{B}_z^{(L)}\rangle/m\gamma$ which corresponds to the rotation of the present frame. Here $\langle\vec{B}_z^{(L)}\rangle$ denotes the guiding synchrotron field.

3. Solution of Spin Equation in Each Element

Solution of the spin equation becomes pretty simple in each element and is presented in Table 1 in a form of the transfer matrix Σ defined by

$$\begin{pmatrix} s_x \\ s_y \\ s_z \end{pmatrix}_{out} = \Sigma \cdot \begin{pmatrix} s_x \\ s_y \\ s_z \end{pmatrix}_{in}$$

where the suffices in and out indicate the entrance to and exit from each element respectively. In each element whose length is much smaller than the unit betatron wave-length, the transverse coordinates of particles are approximated to be constant in calculating Σ. We show below a derivation of the matrices Σ for a few typical elements.

Bending Magnets

Subtracting from (2) a term $e\langle\vec{B}_z^{(L)}\rangle/m\gamma$ and neglecting a small difference $B_z^{(L)} - \langle B_z^{(L)}\rangle$ which is much smaller than $\gamma G\, B_z^{(L)}$, we have the equation of spin motion in the turning rest frame as

$$\frac{d\vec{s}}{dt^{(R)}} = \frac{e}{m}\,\vec{s} \times \{(1 + G)\vec{B}_y^{(L)} + (1 + \gamma G)\vec{B}_x^{(L)} + \gamma G\, \vec{B}_z^{(L)}\} \tag{3}$$

As the fringing region is treated separately, the longitudinal field $\vec{B}_y^{(L)}$ is neglected here.

The solution of (3) is as follows:

$$\begin{cases} s_x(t^{(R)}) = (aQ/A)\{\cos\alpha - \cos(At^{(R)} + \alpha)\} + (s_x)_0\,, \\ s_y(t^{(R)}) = Q\sin(At^{(R)} + \alpha), \\ s_z(t^{(R)}) = (bQ/A)\,\{\cos(At^{(R)} + \alpha) - \cos\alpha\} + (s_z)_0\,, \end{cases} \tag{4}$$

where

$$\begin{cases} a = e\gamma G\, B_z^{(L)}/m\,, \\ b = e(1 + \gamma G)B_x^{(L)}/m\,, \\ A = (a^2 + b^2)^{1/2}\,, \\ Q\sin\alpha = (s_y)_0\,, \\ Q\cos\alpha = \{(bs_z - as_x)/A\}_0\,. \end{cases} \tag{5}$$

Putting $\omega = At^{(R)}$ with $t^{(R)}$ the transit time through the magnet, we have the transfer matrix Σ as shown in Table 1.

Edge Effects of Bending Magnets

Only an impulse of longitudinal field $\vec{B}_y^{(L)}$ is assumed here. Vertical fields can well be described by bending magnets and are neglected here. The equation of spin motion becomes from (2)

$$\frac{d\vec{s}}{dt^{(R)}} = \frac{ge}{2m}\vec{s} \times \vec{B}_y^{(L)}. \tag{6}$$

The solution is given by

$$\begin{cases} s_x(t^{(R)}) = (s_x)_0 \cos(at^{(R)}) - (s_z)_0 \sin(at^{(R)}), \\ s_y(t^{(R)}) = (s_y)_0 , \\ s_z(t^{(R)}) = (s_x)_0 \sin(at^{(R)}) + (s_z)_0 \cos(at^{(R)}), \end{cases} \tag{7}$$

where $a = geB_y^{(L)}/2m$.

Taking an approximation of $B_z^{(L)}$ falling linearly with the distance from the end plane of bending magnet, we have

$$B_y^{(L)} = z\frac{dB_z^{(L)}}{dy} \approx \eta\ z(B_z^{(L)})_{max}/\delta \tag{8}$$

where $(B_z^{(L)})_{max}$ is the field inside the magnet, δ the longitudinal length of fringing region and $\eta = +1$ (or -1) for the entrance (or exit). Then, $at^{(R)}$ ($t^{(R)}$: the transit time over the fringing region) no more depends on δ:

$$at^{(R)} = \eta\frac{gez}{2m\gamma\beta c}(B_z^{(L)})_{max}. \tag{9}$$

The fringing region can, therefore, be taken negligibly thin in consistency with a thin lens approximation in the orbit calculation.

Accelerating Gap

In the particle rest system, a magnetic field $\vec{B}^{(R)}$ arises by applying a Lorentz transformation to a laboratory electric field $\vec{E}^{(L)}$:

$$\begin{cases} B_x^{(R)} \approx -\gamma\beta(E_z^{(L)} - E_y^{(L)} \frac{dz}{dy}) , \\ B_y^{(R)} \approx 0, \\ B_z^{(R)} \approx \gamma\beta(E_x^{(L)} - E_y^{(L)} \frac{dx}{dy}). \end{cases} \tag{10}$$

Here dz/dy and dx/dy are the small angles in the vertical and horizontal directions respectively which the particle trajectory makes with respect to the equilibrium orbit. One can take an effective laboratory field $\vec{B}^{(L)}_{x,z} = \vec{B}^{(R)}_{x,z}/\gamma$ instead of the electric field. As the effect of an energy gain on the spin motion is small, the laboratory electric field $\vec{E}^{(L)}$ is approximately equivalent to the laboratory magnetic field $\vec{B}^{(L)}$ given above, as far as the spin motion is concerned.

The equation of spin motion (2) then becomes [11)]

$$\frac{d\vec{s}}{dt^{(R)}} = \frac{e\beta}{m} (1 + \gamma G) \vec{s} \times \{-(E_z^{(L)} - E_y^{(L)} \frac{dz}{dy})\hat{x} + (E_x^{(L)} - E_y^{(L)} \frac{dx}{dy})\hat{z} \} \tag{11}$$

where $\hat{x}$ (or $\hat{z}$) is the unit vector in the direction x (or z). The above equation is of a similar form as (3). The solution is given by (4) with a and b redefined as

$$\begin{cases} a = \frac{e\beta}{m} (1 + \gamma G)(E_x^{(L)} - E_y^{(L)} \frac{dx}{dy}) \\ b = \frac{-e\beta}{m} (1 + \gamma G)(E_z^{(L)} - E_y^{(L)} \frac{dx}{dy} \end{cases} \tag{12}$$

4. Computation

The accelerator ring consists of eight cells and has the following numbers: injection (or maximum) kinetic energy = 20.8 (or 500) MeV, bending (or average) radius = 3.3 (or 6) m, betatron wave number $\nu_z = \nu_x = 2.25$, and n-value = 12.091. The repetition rate is 20 pulses per sec. The magnet excitation is sinusoidal with the accelerating time of about 18 msec.

The structure of unit cell is $\frac{1}{2}$OFDDF$\frac{1}{2}$O in the horizontal plane, where O indicates a straight section, F a focusing sector and D a defocusing one. Magnetic field distribution on the equilibrium orbit is taken flat inside a magnet sector, falling to zero linearly with the distance from the edge. The magnetic sectors are treated in the sharp edged approximation. The longitudinal field in the fringing region is treated in the thin lens approximation at the edge. Edge effects between adjacent F and D sectors almost completely cancel out each other and are neglected. These simplifying approximations give a slightly different number of ν_z from the experimental one of 2.25. In order to obtain $\nu_z = 2.25$, the lengths of magnetic sectors are slightly modified from the actual ones (see Fig. 2).

The r.f. acceleration is made in one of the eight straight sections. Though two accelerating gaps exist in the same straight section, we approximate them by one gap placed in the centre of the straight section. The adiabatic damping for betatron oscillations is taken into account at the accelerating gap by a shrinkage in the orbit divergence in proportion to $(\text{momentum})^{-1}$.

Computational Results

The final polarization at 500 MeV is presented in Fig. 3 as a function of the vertical oscillation amplitude z_{max} of particle at the resonance. The initial polarization at 20 MeV is +1.0 in the vertical direction. Complete spin flip occurs if z_{max} is larger than 3 mm. The final polarization hardly changes, in agreement with a theoretical expectation, even if the radial oscillation amplitude is widely changed.

Variations of the polarization in the course of acceleration are presented in Fig. 4 for three typical particles. No depolarization is seen except at the resonance.

From Fig. 3 one can estimate the final beam polarization by assuming a uniform distribution of particles in the phase space. Fig. 5 gives the final beam polarization as a function of the maximum of the vertical beam radius at the resonance. For a beam radius of 10 mm, the final beam polarization is higher than -0.98.

Comparison between Computation and Analytical Formula

Let us compare the computed depolarization with an analytical formula[2)]

$$\begin{cases} P/P_0 = 1 - \exp(-X) \\ X = [\pi(1 + \gamma G)r]^2/G\Delta\gamma \end{cases} \qquad (13)$$

where P (or P_0) is the final (or initial) polarization, $\Delta\gamma$ the increment of γ per revolution and $r = z_0\nu_z^2/2R_{av}$ (here R_{av} = average ring radius; z_0 = the amplitude of $\cos(\nu_z\theta)$ component of vertical betatron oscillation at the resonance). For the present case $\gamma = 1.255$ and $\Delta\gamma = 8.7 \times 10^{-6}$. Fitting the betatron oscillation by

$$z = z_0\cos(\nu_z\theta + \phi_z)\ \{1 + \sum_{m=1}^{\infty} z_m\cos(8m\theta)\} \qquad (14)$$

we find $z_0 = 0.71\ z_{max}$. We have then $r = 0.30 \times 10^{-3} z_{max}$(in mm) and $X = 0.60 z_{max}^2$(in mm). The final polarization given by (14) agrees well with the computed one.

5. Influence of Synchrotron Oscillation

Only the synchronous particles have been treated throughout the above computation. The synchrotron oscillation has two effects.[6,12,13]

First, the synchrotron oscillation modulates the crossing speed across the resonance. By comparing the peak accelerating voltage of 16 kV with 8.5 kV for the synchronous particles, the maximum crossing speed is twice that for synchronous particles. This effect is roughly equivalent to a decrease in the horizontal field (i.e. the vertical beam size) by a factor of $1/\sqrt{2}$ with the crossing speed as before, as seen in (13). If the maximum crossing speed is assumed for half amount of particles, the final polarization changes from -0.98 to -0.97 as seen from Fig. 5.

Second, the synchrotron oscillation may cause multiple crossing across the same resonance energy. The synchrotron oscillation at the resonance has the following paramaters: the synchronous phase $\sim 30°$, the stability region $\sim -30° - +90°$ and the frequency $\sim$ 10 kHz. From the shape of the longitudinal phase space three quarters of particles may experience decelerating fields. From the peak and average accelerating voltages, less than 2/7 of particles may cross the resonance three times, if they have the maximum amplitude of synchrotron oscillation.

Combining the above two numbers, and reducing the result by half because the synchrotron oscillation amplitude is distributed between zero and the maximum, we find that less than 10 % of particles may cross the resonance three times. If we assume a worst case that the multiple crossing might destroy the polarization completely, the polarization loss is less than 10 %.

Summing up the above two effects, we may expect that an additional polarization loss due to synchrotron oscillation is actually much smaller than 10%.

6. Reducing the Depolarization by a ν_z-Jump Technique

Instead of the complete spin flip, we may employ a ν_z-jump technique to maintain the initial polarization including the sign. A computed result is shown in Figs. 3 and 5 by dotted lines for a case of pulsing 10 cm thick (effective thickness) quadrupole magnets added on both ends of each straight section up to 0.1 kGauss/cm within 3 μsec (see Fig. 7). The fall time of excitation pulse is take[illegible], to which the result is not so sensitive. The change of ν_z is 0.12. A typical variation of the polarization with respect to energy is shown in Fig. 8. If the beam radius is 10 mm at the resonance, the depolarization is as small as 6 %. Influence of synchrotron oscillation is negligibly small because the change in ν_z is much faster than the oscillation in γG.

7. Conclusions

The beam polarization is expected to flip almost completely at 239 MeV, the only intrinsic resonance in the KEK 500 MeV booster PS. For the initial beam polarization of +1.0, the final beam polarization is as high as -0.98 (or -0.92) if the beam radius is 10 mm (or 6 mm) at the resonance, and if synchrotron oscillation is neglected. Though synchrotron oscillation may cause an additional polarization loss, it is smaller than 10 %.

If a ν_z-jump technique is employed the initial polarization may be maintained including the sign. The depolarization will be as small as 6 % by pulsing 10 cm thick quadrupole magnets added on both ends of each straight section up to 0.1 kGauss/cm within 3μμsec. In this case the influence of synchrotron oscillation is negligibly small.

Acknowledgements

The author should appreciate Professor K. Morimoto and Dr. T. Suzuki for very helpful discussions on the spin as well as orbit motion, and Professor S. Takeda on the r. f. acceleration. He is also deeply thankful to members of the Data Handling Division at KEK for aids.

References

1) T. K. Khoe: "Acceleration of Polarized Protons in the KEK Synchrotron" KEK-73-8 (1973)

2) T. Khoe et al: Particle Accelerators 6 (1975) 213
E. F. Parker: IEEE NS-22 (1975) 1466

3) H. Sasaki: "Acceleration of Polarized Protons by KEK Synchrotron" U. S. - Japan Seminar on High Energy Accelerator Science, Tokyo and Tsukuba (KEK, 1973) p. 247

4) J. Faure, A. Hilaire and R. Vienet: Particle Accelerators 3 (1972) 225

5) L. C. Teng: "Depolarization of a Polarized Proton Beam in a Circualr Accelerator" FN-267-0100 (1974)

6) M. Kobayashi: "Spin Flip by Adiabatic Passage of Depolarizing Resonances in Synchrotrons" to be presented elsewhere.

7) D. Cohen: Rev. Sci. Instr. 33 (1962) 161

8) Kh. A. Simonian: "Numerical-Analytical Calcülation of the Acceleration of the Polarized Electrons in Synchrotron" V-th Intern. Conf. on High Energy Accelerators (Frascati, 1965) p. 572

9) M. Froissart and R. Stora: Nucl. Instrum. Meth. 7 (1960) 297

10) E. Grorud, J. L. Laclare and G. Leleux: "Resonances de Depolarisation dans Saturne 2" GOC-GERMA 75-48/TP-28 (1975)

11) In the limit of $\beta = 1$ and $E_x = E_y = 0$, Eq. (11) coincides with a formula given by Chao. A. W. Chao: "Depolarization Calculation Using Generalized Matrices" SPEAR-208/PEP-257 (1977)

12) Y. Cho et al: "Phenomena Associated with the Acceleration of Polarized Protons in Circular Accelerators" 1976 Conf. on H. E. Physics with Polarized Beams and Targets, ANL, 1976, p. 396

13) A study is also made by S. Huramatsu and Y. Mori: see a report of S. Suwa, III Int. Symp. H. E. Phys. with Polarized Beams and Targets, ANL, 1978.

Figure Captions

Fig. 1 The turning rest frame of particles, (xyz).

Fig. 2 Structure of the unit cell. Lengths are in m. T shows transition sectors. In computations, the following lengths are used to give $\nu_z = 2.250$ by neglecting the transition sectors (see text): 0.65311 m for F and 0.64279 m for D. These lengths give ν_x = 2.229 (the d sign value ∿ 2.25).

Fig. 3 The final polarization of particles as a function of the amplitude of vertical betatron oscillation z_{max} at the resonance. The dotted curve is obtained if a ν_z-jump technique is employed (see text).

Fig. 4 Typical variations of polarization with respect to the kinetic energy of particles. The amplitude of vertical betatron oscillation z_{max} at the resonance is: (a) 1.1 mm, (b) 2.9 mm and (c) 30 mm.

Fig. 5 The final polarization of beam as a function of the maximum of the vertical beam radius at the resonance. The dotted curve is obtained if a ν_z-jump technique is employed (see text).

Fig. 6 A scheme of ν_z-jump technique employed in computation. $\delta\gamma_r$ = 0.000125 (3 μsec), $\delta\gamma_f = 500\ \delta\gamma_r = 0.0625$ and $\delta\nu_z = 0.12$.

Fig. 7 A typical variation of polarization with respect to the kinetic energy of particle when a ν_z-jump technique (see Fig. 6) is employed. The amplitude of vertical betatron oscillation z_{max} at the resonance is 10 mm.

Table 1 Transformation matrix for spin vector*

	Σ	Notes
Fringing Region of Bending Magnet	$\begin{pmatrix} \cos\omega, & 0, & -\eta\sin\omega \\ 0 & 1 & 0 \\ \eta\sin\omega & 0 & \cos\omega \end{pmatrix}$	$\omega=\frac{gezB_0}{2m\gamma\beta c}$
Fringing Region of Q-Magnet	$\eta=+1(-1)$ for entrance(exit)	$\omega=\frac{gexzG_Q}{2m\gamma\beta c}$
Bending Magnet (Hor. Focusing Sector)	$\begin{pmatrix} \frac{a^2\cos\omega+b^2}{A^2}, & \frac{a\sin\omega}{A}, & \frac{ab(1-\cos\omega)}{A^2} \\ \frac{-a\sin\omega}{A}, & \cos\omega, & \frac{b\sin\omega}{A} \\ \frac{ab(1-\cos\omega)}{A^2}, & \frac{-b\sin\omega}{A}, & \frac{a^2+b^2\cos\omega}{A^2} \end{pmatrix}$	$a=\frac{e\gamma GB_0}{m}(1+\frac{nx}{\rho})$, $b=\frac{e(1+\gamma G)B_0nz}{m\rho}$
Bending Magnet (Hor. Defocusing Sector)		$a=\frac{e\gamma GB_0}{m}(1-\frac{nx}{\rho})$, $b=\frac{-e(1+\gamma G)B_0nz}{m\rho}$
Q - Magnet		$a=\frac{e}{m}(1+\gamma G)G_Qx$, $b=\frac{e}{m}(1+\gamma G)G_Qz$
Accelerating Gap	$A=(a^2+b^2)^{1/2}$, $\omega=A\ell/\gamma\beta c$	$a=\frac{e\beta}{mc}(1+\gamma G)(E_x-E_y\frac{dx}{ydy})$, $b=\frac{-e\beta}{mc}(1+\gamma G)(E_z-E_y\frac{dz}{ydy})$

*) ℓ = longitudinal length of each region

c = charge (positive for protons)

B_0 = laboratory bending field on the equilibrium orbit (negative)

G_Q = flux density gradient of quadrupole magnets (negative for horizontally focusing quadrupoles)

n = absolute value of the conventional n value

$\vec{E}$ = laboratory accelerating field (E_y : negative)

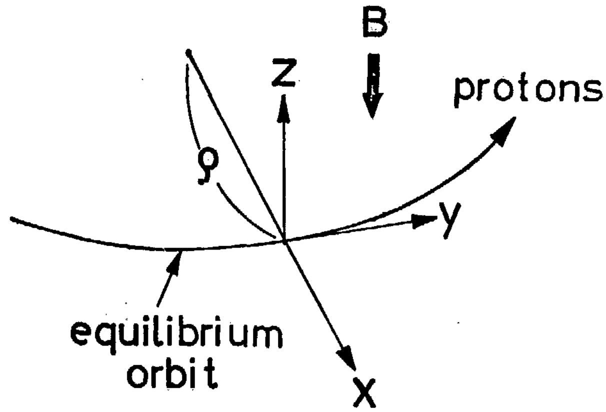
B
z
protons
ϱ
y
equilibrium
orbit
x

Fig. 1

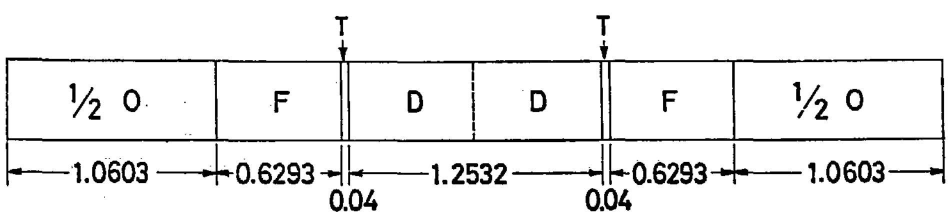
T
T
½ O
F
D
D
F
½ O
1.0603
0.6293
1.2532
0.6293
1.0603
0.04
0.04

Fig. 2

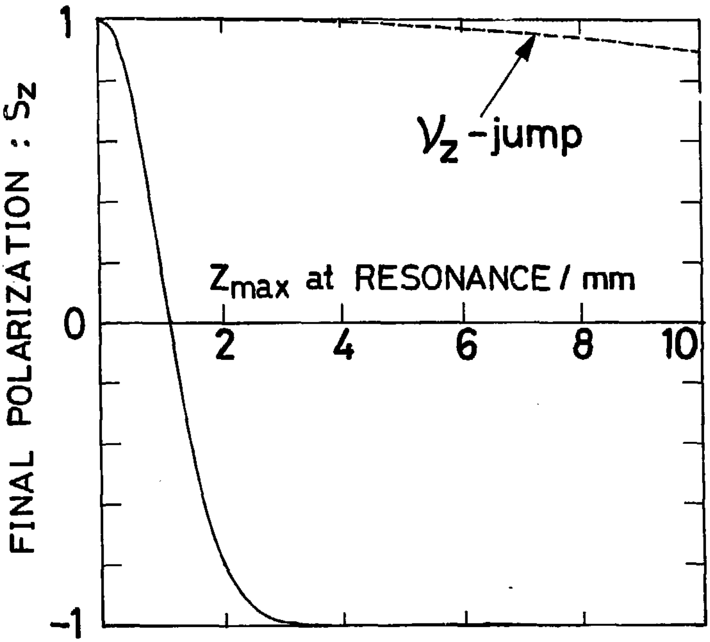
FINAL POLARIZATION : S_z
1
0
-1
ν_z -jump
Z_{max} at RESONANCE / mm
2
4
6
8
10

Fig. 3

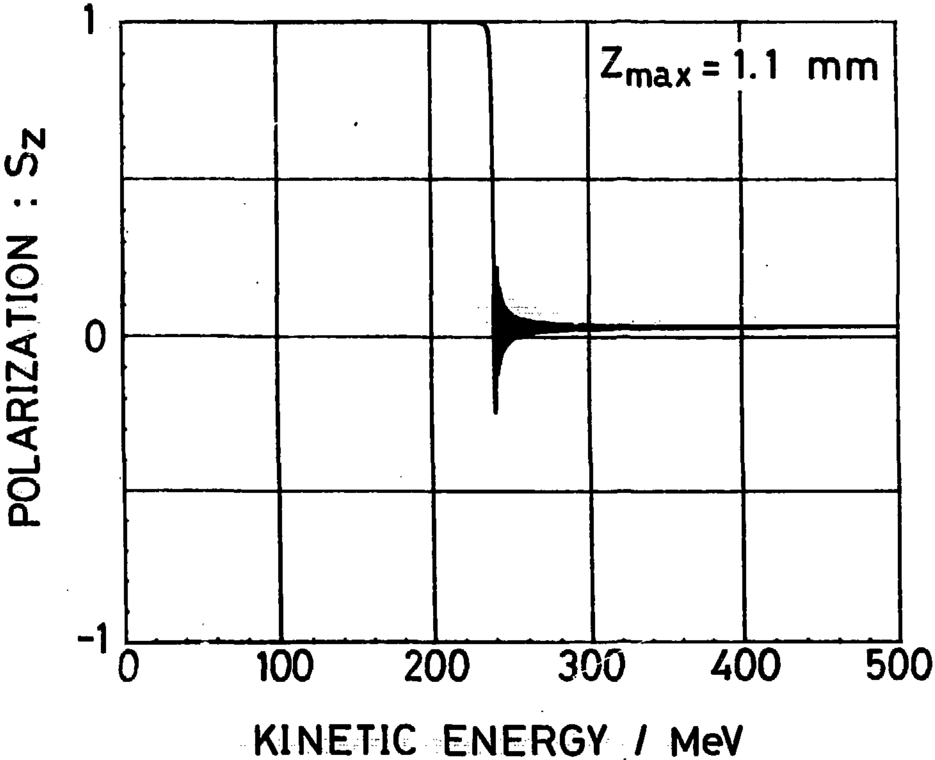

1
0
-1
0
100
200
300
400
500
POLARIZATION : Sz
KINETIC ENERGY / MeV
Zmax = 1.1 mm

Fig. 4(a)

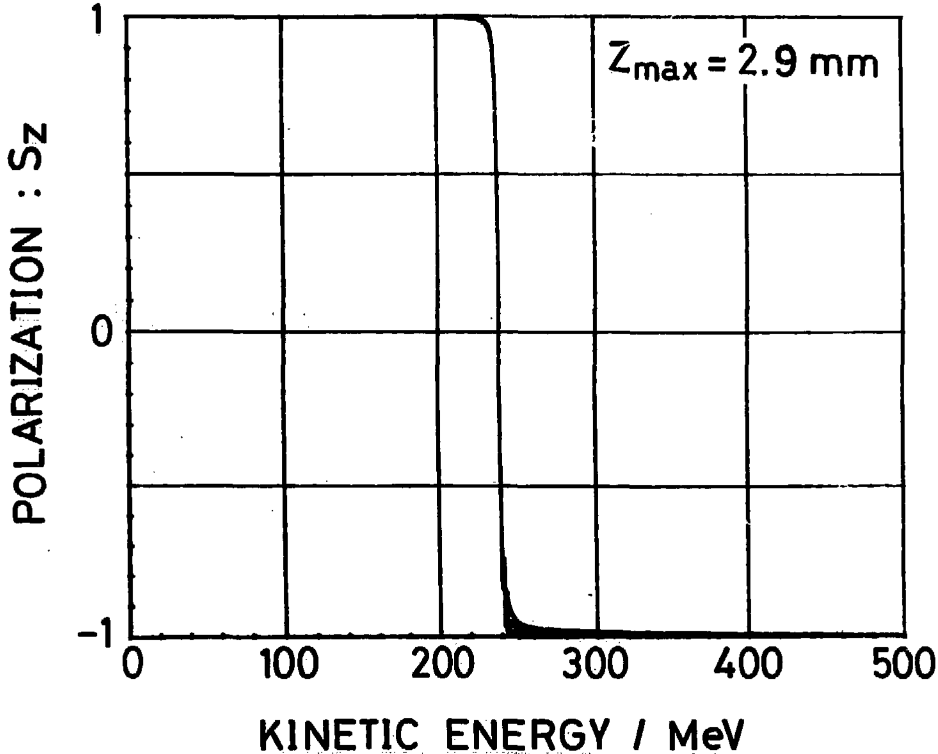
1
0
-1
POLARIZATION : Sz
Zmax = 2.9 mm
0
100
200
300
400
500
KINETIC ENERGY / MeV

Fig. 4(b)

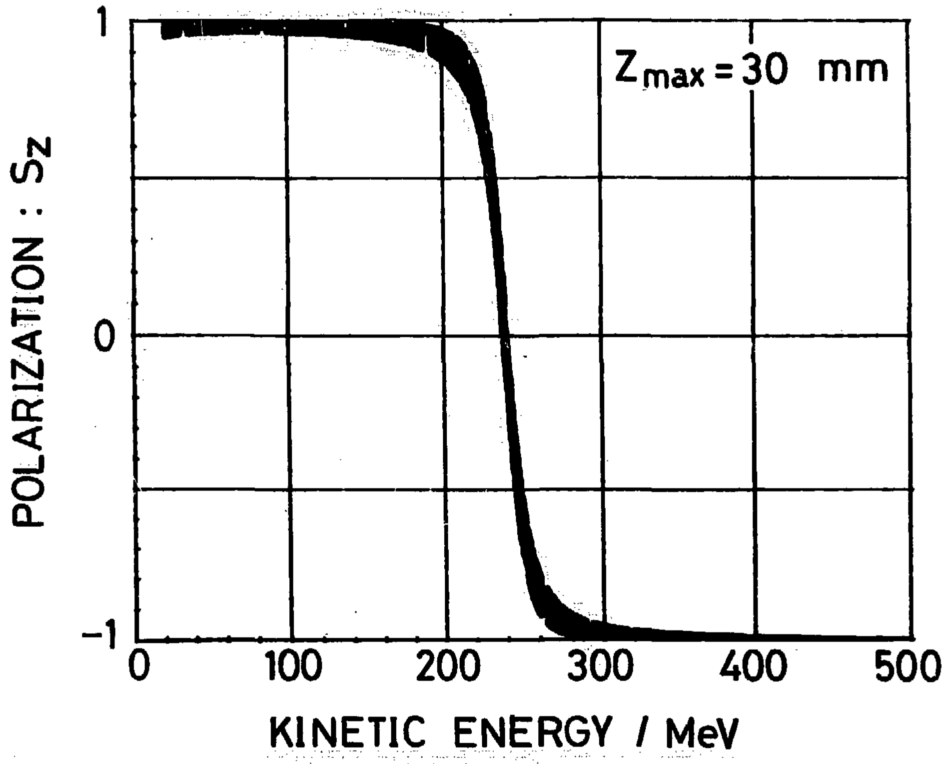
1
0
−1
POLARIZATION : S_Z
Z_{max} = 30 mm
0
100
200
300
400
500
KINETIC ENERGY / MeV

Fig. 4(c)

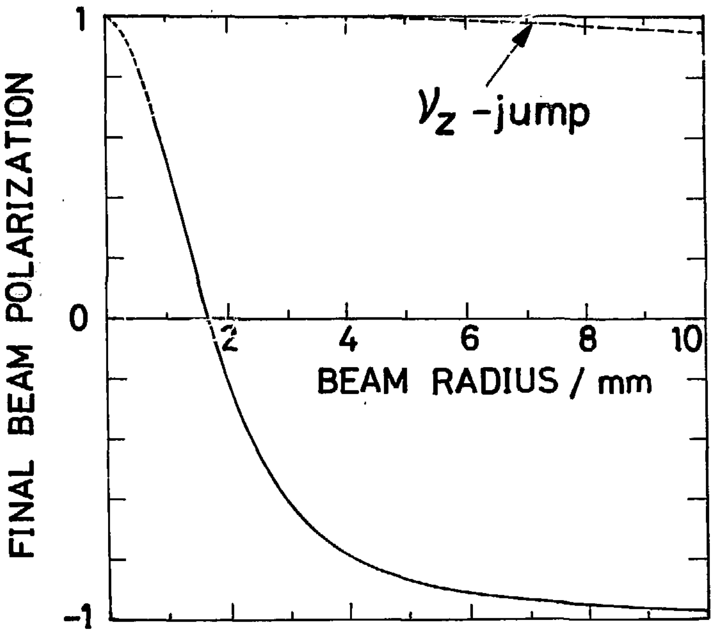
1
0
-1
FINAL BEAM POLARIZATION
γ_z -jump
2
4
6
8
10
BEAM RADIUS / mm

Fig. 5

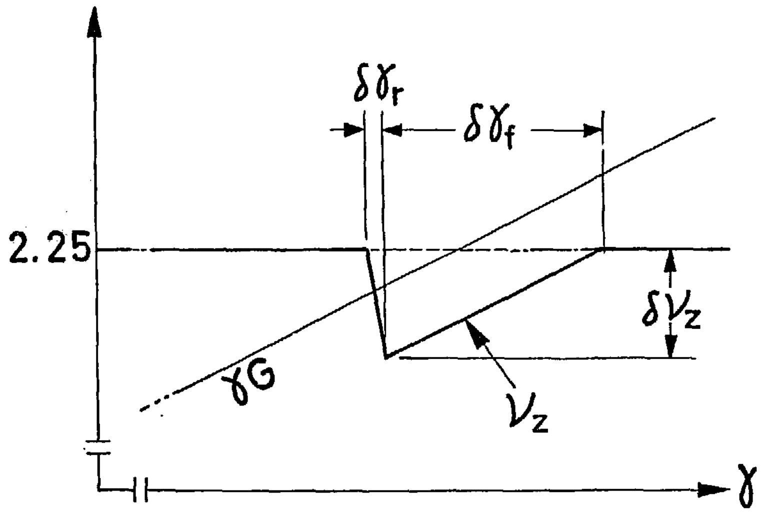
δγr
δγf
2.25
δνz
γG
νz
γ

Fig. 6

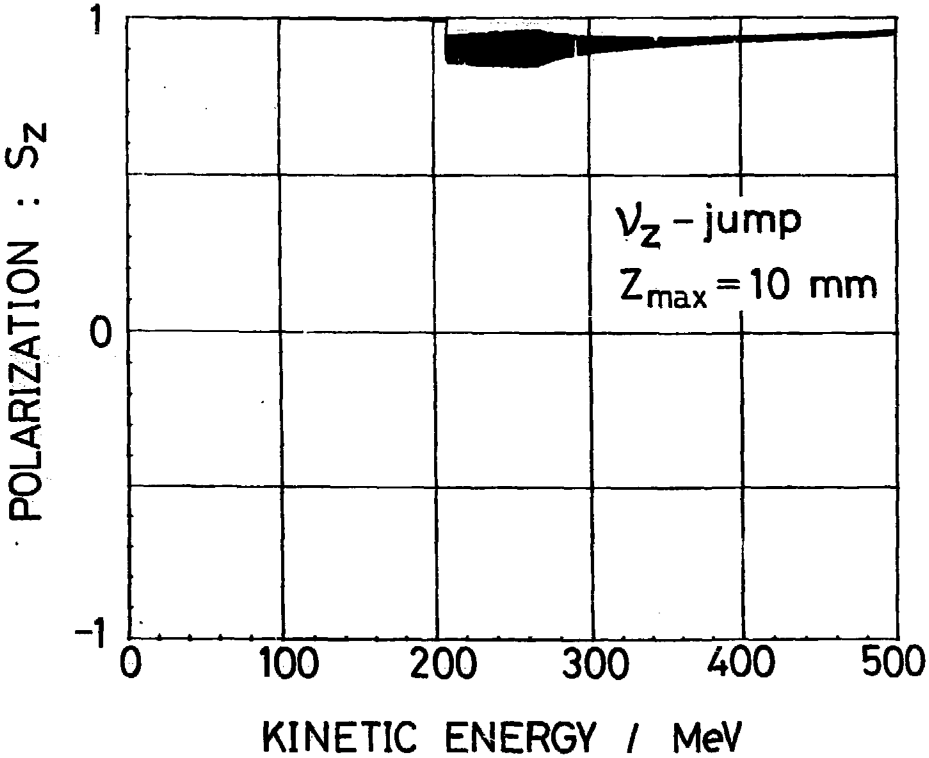
1
0
−1
POLARIZATION : Sz
νz − jump
Zmax = 10 mm
0
100
200
300
400
500
KINETIC ENERGY / MeV

Fig. 7